

R-Process Abundances and Chronometers in Metal-Poor Stars

John J. Cowan,¹ B. Pfeiffer,² K.-L. Kratz,² F.-K. Thielemann,³ Christopher Sneden,⁴ Scott Burles,^{5,6} David Tytler,⁵ and Timothy C. Beers⁷

cowan@mail.nhn.ou.edu, pfeiffer@vkcmzd.chemie.uni-mainz.de,
klkratz@vkcmzd.chemie.uni-mainz.de, fkt@quasar.physik.unibas.ch,
chris@verdi.as.utexas.edu, scott@riigoletto.uchicago.edu, tytler@ucsd.edu,
beers@pa.msu.edu

To appear in *The Astrophysical Journal*, **521**

Received _____; accepted 18 March 1999

¹Department of Physics and Astronomy, University of Oklahoma, Norman, OK 73019

²Institut für Kernchemie, Univ. Mainz, Fritz-Strassmann- Weg 2, D-55099 Mainz, Germany

³Department für Physik und Astronomie, Univ. Basel, Klingelbergstr. 82, CH-4056 Basel, Switzerland

⁴ Department of Astronomy and McDonald Observatory, University of Texas, Austin, TX 78712

⁵Department of Physics and Center for Astrophysics and Space Sciences, University of California, San Diego, MS 0424, La Jolla, CA 92093-0424

⁶Department of Astronomy and Astrophysics, University of Chicago, Chicago, IL 60637

⁷Department of Physics and Astronomy, Michigan State University, E. Lansing, MI 48824

ABSTRACT

Rapid neutron-capture (i.e., r -process) nucleosynthesis calculations, employing internally consistent and physically realistic nuclear physics input (QRPA β -decay properties and the recent ETFSI-Q nuclear mass model), have been performed. These theoretical computations assume the classical waiting-point approximation of $(n,\gamma) \rightleftharpoons (\gamma,n)$ equilibrium. The calculations reproduce the solar isotopic r -abundances in detail, including the heaviest stable Pb and Bi isotopes. These calculations are then compared with ground-based and HST observations of neutron-capture elements in the metal-poor halo stars CS 22892–052, HD 115444, HD 122563 and HD 126238. The elemental abundances in all four metal-poor stars are consistent with the solar r -process elemental distribution for the elements $Z \geq 56$. These results strongly suggest, at least for those elements, that the relative elemental r -process abundances have not changed over the history of the Galaxy. This indicates also that it is unlikely that the solar r -process abundances resulted from a random superposition of varying abundance patterns from different r -process nucleosynthesis sites. This further suggests that there is one r -process site in the Galaxy, at least for elements $Z \geq 56$.

Employing the observed stellar abundances of stable elements, in conjunction with the solar r -process abundances to constrain the calculations, predictions for the zero decay-age abundances of the radioactive elements Th and U are presented. We compare these predictions (obtained with the mass model ETFSI-Q, which reproduces solar r -abundances best) with newly derived observational values in three very metal-poor halo stars: HD 115444, CS 22892–052 and HD 122563. Within the observational errors the ratio of [Th/Eu] is the same in both CS 22892–052 and HD 115444. Comparing with the theoretical ratio

suggests an average age of these two very metal-poor stars to be 15.6 ± 4.6 Gyr, consistent with earlier radioactive age estimates and recent globular and cosmological age estimates. Our upper limit on the uranium abundance in HD 115444 also implies a similar age. Such radioactive age determinations of very low metallicity stars avoid uncertainties in Galactic chemical evolution models. They still include uncertainties due to the involved nuclear physics far from beta-stability. However, we give an extensive overview of the possible variations expected and come to the conclusion that this aspect alone should not exceed limits of 3 Gyr. Therefore this method shows promise as an independent dating technique for the Galaxy.

Subject headings: Galaxy: evolution — nuclear reactions, nucleosynthesis, abundances — stars: abundances — stars: individual (CS 22892–052, HD 115444, HD 122563, HD 126238) — stars: Population II

1. Introduction

Elemental abundances in metal-poor halo stars provide important clues to the chemical evolution of the early Galaxy. Since these stars are extremely old, their abundance patterns are living records of the first generations of Galactic nucleosynthesis. Much recent observational and theoretical work has concentrated on understanding the origin of neutron-capture elements in halo stars. These elements are those with atomic numbers $Z > 30$ (or mass numbers $A > 68$), thus comprising the majority of elements in the periodic table. Some isotopes of the neutron-capture elements may be built through neutron bombardment rates that are slow enough to allow all beta-decays to take place between successive neutron captures; this is called the *s*-process. Alternatively, short-duration rapid neutron bombardments that occur more rapidly than beta-decay rates can produce other neutron-capture element isotopes; this is the *r*-process. More generally, many isotopes may arise from a combination of both *s*- and *r*-processes, and great care must be exercised in determining the relative contributions of each of these processes to the solar and stellar elemental abundances.

Many chemical composition studies of low-metallicity stars have detected the presence of a strong *r*-process component in the neutron capture element abundances (Spite & Spite 1978, Truran 1981, Sneden & Parthasarathy 1983, Sneden & Pilachowski 1985, Gilroy et al. 1988, Gratton & Sneden 1991, 1994; Sneden et al. 1994; McWilliam et al. 1995a, 1995b; Cowan et al. 1996, Sneden et al. 1996, Burris et al. 1998; McWilliam 1998). In addition, there has been increasing evidence suggesting a relative or scaled solar *r*-process abundance pattern in these stars, at least for the heaviest of these elements (Gilroy et al. 1988, Cowan et al. 1995, Sneden et al. 1996, Cowan et al. 1997).

Even though the elemental abundance patterns apparently are in agreement with a purely solar *r*-process distribution, these are necessarily sums over individual isotopic

abundances. Therefore a successful solar r -process match to stellar elemental abundances still gives fewer constraints to their isotopic composition than would a direct observation of a solar isotopic r -process abundance pattern. In principle, there exists a degeneracy in the sense that different non-solar isotopic abundance patterns might still fit a solar r -process elemental pattern. It is theoretically possible to produce identical abundances for approximately 30 elements with $Z \geq 56$ through different mixtures of the approximately 80 individual isotopes of these elements. It is harder to do this with superpositions from different r -process calculations. Goriely & Arnould (1997) have shown that a series of several non-solar isotopic abundance distributions could produce a total elemental abundance pattern that indeed matches closely some of the neutron-capture elements in one low-metallicity star, especially those in the more insensitive relatively flat regions in between r -process peaks. However, if also the peaks have to be reproduced at their precise locations (and there exists an increasing amount of data in the Pt peak), this agreement can no longer occur as a result of any random superposition of abundances. There has to be an intriguing conspiracy for compensation of the non-solar values of different isotopes in order to still fit a solar element composition. The most reasonable explanation is that the same set of superpositions occurs in each individual event. This would also explain why such a pattern is already observed in the lowest metallicity stars, where only one or at most a few events contributed. Thus, while the observation of a solar r -process elemental pattern in certain mass regions is not an absolute proof for isotopic solar r -process abundances, it is the most reasonable and probable conclusion when also the peaks have to be reproduced correctly.

This conclusion is further strengthened by the existence of a scaled solar r -process abundance pattern for many elements, not just in one low-metallicity star, but now in four stars (Sneden et al. 1996, 1998). The data for these stars are not restricted to a narrow region of elements (i.e., the rather flat inter-peak region near mass number 150), but now

cover a wide elemental range from Ge ($Z = 32$) through Pb ($Z = 82$). These recently observed abundance patterns also agree with earlier findings, for a wide range of stars with varying metallicities, that the Ba/Eu ratio varies from a pure r -process ratio at low metallicities to a solar mix at solar metallicities (see McWilliam’s 1997 review and references therein; also McWilliam 1998, Burris et al. 1998). Magain (1995) recently attempted to estimate Ba isotopic abundances from synthetic/observed profile comparisons of a Ba II line in the very low-metallicity subgiant HD 140283. He concluded that a total solar system isotopic mix (i.e., r - + s -process) provided the best match, implying a significant s -process contribution to the neutron-capture elements in this star. However, François & Gacquer (1999) have repeated Magain’s investigation with superior spectroscopic data, and derive an isotopic mix for this same star that is consistent with a purely r -process synthesis origin.

There have been several difficulties, however, in determining the true nature of the stellar abundance pattern. First, most of the stellar abundance determinations already exist for the easily observed rare-earth elements, but these elements occur between the 2nd and 3rd neutron-capture peaks, i.e., in the relatively flat inter-peak region. The second r -process peak (near mass number, A , ~ 130) contains such elements as Te and Xe that at present have no identifiable solar and stellar transitions. The 3rd solar peak ($A \sim 195$, with elements Os, Ir and Pt) has mostly UV transitions and is thus not accessible to ground-based observations.

Additionally, there have been theoretical difficulties in predicting the neutron-capture element abundances. The first of these is the well-known uncertainty in the site of the r -process (see Cowan, Thielemann, & Truran 1991, Mathews, Bazan, & Cowan 1992, Meyer 1994 for further discussion of possible sites). Even promising scenarios, like the high entropy neutrino wind in supernovae (Takahashi, Witt, & Janka 1994, Woosley et al. 1994, Qian & Woosley 1996) have problems in obtaining the required entropies, and they have deficiencies

in their abundance predictions (Freiburghaus et al. 1999, Meyer, McLaughlin, & Fuller 1998). Thus, even though it would be preferred, it is currently not possible to provide results from a specific r -process site which give a good global fit to the observed, stable solar r -process abundances. Heretofore only observed stellar and scaled solar abundances have been compared. Therefore, at the very least we need to develop tools to theoretically predict “zero-age” solar r -process abundances for those long-lived unstable neutron-capture elements, where the solar abundances have been modified by decay from the initial zero-age abundances produced in an r -process site. The abundances of the stable elements in, and beyond, the 3rd r -process peak (up to $A=209$) can be used to help constrain the predictions of such an initial production pattern of the nuclei with $A > 209$, because the mass numbers 206, 207, 208, and 209 contain large contributions from several alpha-decay chains of heavier nuclei. This helps especially to predict the long-lived radioactive chronometers Th and U, independent of knowing the site for the r -process.

A final problem is that the nuclei involved in the r -process are far from stability and therefore the requisite nuclear data needed for reliable r -process predictions are in most cases not obtainable by experimental determination. However, there have been recent advances in theoretical prescriptions for very neutron-rich nuclear data (Möller et al. 1995, Aboussir et al. 1995, Möller, Nix, & Kratz 1997, Chen et al. 1995, Pearson, Nayak, Goriely 1996).

The detection of thorium in the ultra-metal-poor halo star CS 22892-052 (Sneden et al. 1994, Sneden et al. 1996, Cowan et al. 1997) in conjunction with the HST detections of the third r -process peak elements in some halo stars bears directly on nucleochronology. The long-lived radioactive nuclei (known as chronometers) in the thorium-uranium region are formed entirely in the r -process and can be used to determine the ages of stars and the Galaxy. In other low-metallicity stars the detection of neutron-capture elements in the

(osmium-platinum) 3rd r -process peak, a nuclear region near that of uranium and thorium, confirms the full operation of the r -process for the synthesis of the heaviest ($Z > 55$) r -process elements during the early history of the Galaxy.

The combination of the improved nuclear and stellar data will now allow more comprehensive and detailed attempts at a determination of the nature of the abundance patterns in these earliest Galactic stars. In this paper we analyze the production of the r -process elements in the solar system and in four metal-poor halo stars. In §2 we describe the r -process calculations and their relevance to the solar system isotopic abundance mix. Abundance comparisons between the calculations and the recent observations of four different metal-poor halo stars are made in §3. Age estimates, based upon predicted and observed radioactive chronometers in the stars CS 22892–052 and HD 115444 (and therefore also lower limits for the Galactic age), are given in §4. In §5 we conclude with a discussion of our results.

2. Calculations

We assume, as a working hypothesis, that the heavy element abundances of very low metallicity stars are given by a pure r -process composition. This assumption is supported by the observational evidence, at least for the elements beyond Ba, where data are available. We have analyzed r -process abundances with predictions from calculations in the waiting-point assumption (or $(n,\gamma) \rightleftharpoons (\gamma,n)$ equilibrium) with a continuously improving nuclear data base (Kratz et al. 1988, Kratz et al. 1993, Thielemann et al. 1994, Chen et al. 1995, Pfeiffer et al. 1997). This approach is based on a continuous superposition of r -process components with a varying r -process path related to contour lines of neutron separation energies in the range of 4 to 2 MeV; the latter being determined by the combination of neutron number density and temperature. Such a procedure is also site-independent and

essentially meant to provide a good fit to solar r -abundances, but it can also provide information regarding the type of conditions that a “real” r -process site has to fulfill. The fit is performed by adjusting the weight of the individual components for different neutron separation energies $S_n(n_n, T)$ and the time duration τ for which these (constant) conditions are experienced, starting with an initial abundance in the Fe-group. For a given (arbitrary) temperature, T , S_n is a function of neutron number density, n_n . The superposition weights $\omega(n_n)$ and process durations $\tau(n_n)$ have a behavior similar to powers of n_n . This corresponds to a linear relation in $\log(n_n)$ and is already observed when taking a minimum of three components in order to fit the $A=80$, 130 , and 195 abundance peaks (Kratz et al. 1993). This approach (although only a fit and not a realistic site calculation) also has the advantage that such a continuous dependence on physical conditions has embedded some relation to an (although unknown) astrophysical site. Therefore, one expects some predictive power also for mass regions that are not explicitly fitted.

This technique should be preferable to a multi-event superposition of components with a permitted random relation between ω , τ and n_n (Goriely & Arnould 1996). In such a case, it is (similar to a Fourier analysis) almost always possible to obtain a good fit for any type of nuclear mass model, but this is achieved by possibly even compensating for deficiencies in nuclear properties. Such an approach is not random but its superpositions can change randomly with different mass models. By employing thousands of components, features within the fit interval can be reproduced very well, but very probably - like for a high power polynomial fit - one expects less predictive power at the boundaries and outside of that fit region. Such a procedure (solution to an inverse problem) is meaningful when essentially all physics is understood and only the superposition scheme has to be unraveled. This is the case for the s -process, involving predominantly stable nuclei. It is thus comforting that Goriely (1997) could reproduce the long utilized exponential superposition of neutron exposures (see e.g. Seeger, Fowler, & Clayton 1965; Käppeler et al. 1989) for the s -process.

This is a strong support for doing so also in r -process analyses, as long as we have to deal with unknown uncertainties in nuclear physics.

Following our simplifying but physically predictive procedure, the best agreement with solar system r -process abundances was obtained when we employed the nuclear mass predictions from an extended Thomas Fermi model with quenched shell effects far from stability (i.e., ETFSI-Q, Pearson, Nayak, & Goriely 1996) and the beta-decay properties from QRPA-calculations based on the methods described in Möller & Randrup (1990; see also Möller et al. 1997). The choice of this quenched mass formula is strengthened by recent experimental results for very neutron-rich isotopes in the ^{132}Sn region (Kratz 1998, Fogelberg et al. 1998). Also comparison of masses around $N=82$ are in better agreement with the ETFSI-Q predictions than with any other commonly used mass formula (Isakov et al. 1998, Mach et al. 1998).

The necessary superposition of different components (with r -process paths of a corresponding neutron separation energy S_n and duration τ) can be expressed in terms of superposition weights $\omega(S_n)$ and durations $\tau(S_n)$. How in the still uncertain astrophysical environments such S'_n s are attained is uncertain and not unique. For an (n, γ) - (γ, n) equilibrium, the maximum in each isotopic chain at a given S_n can be attained for arbitrary combinations of n_n and T . For simplicity (but not uniqueness) we have chosen $T = 1.35 \times 10^9\text{K}$, which makes $S_n(n_n, T)$ only a function of n_n . Then the superposition can also be expressed in the form $\omega(n_n)$ expressed in the form $\omega(n_n) = 8.36 \times 10^6 n_n^{-0.247}$ and $\tau(n_n) = 6.97 \times 10^{-2} n_n^{0.062}$ sec, when restricting the fit to the mass regions around the r -process peaks ($A=80, 130, 195$), where the paths come closest to stability, mass model extrapolations need not be extended far into unknown territory, and even a limited amount of experimental information is available. These power laws in n_n play a similar role as an exponential superposition of neutron exposures in the classical s -process. The $(n, \gamma) \rightleftharpoons$

(γ, n) equilibria on which the r -process calculations are based, will likely be obtained in any astrophysical environment with conditions in excess of $n_n=10^{20} \text{ cm}^{-3}$ and $T = 10^9\text{K}$, as expected from all possible sites (Meyer 1994). The major remaining question is related to the assumption of an $(n, \gamma) \rightleftharpoons (\gamma, n)$ equilibrium during the "freeze-out" phase in realistic astrophysical sites and depends on the temporal decline pattern of neutron density and temperature below the above mentioned limits. Thielemann et al. (1998) and Freiburghaus et al. (1999) could show with full network calculations, and without an a priori assumption of equilibria, that these freeze-out effects are small, when mass models which include shell quenching far from stability are used. They also showed that the smooth superposition of results from different neutron separation energies with declining weights for smaller S_n -values can be translated into an almost constant entropy superposition of full network calculations for masses with $A > 110$ (see also Figure 2 and the discussion in Takahashi et al. 1994). The coefficients and powers were obtained from a least square fit to solar r -abundances with the nuclear input discussed above.

We have used this physically motivated fitting procedure, which apparently reproduces the stable solar r -process abundances very well with a simple and robust superposition scheme, for the calculations in this paper. The similarity to the well known and tested classical s -process approach of an exponential superposition of neutron exposures provides a further support for its application. It has the additional advantage that it leads to clear predictions which have to and can be tested. Therefore, in the present investigation we have extrapolated the calculations into unknown territory, specifically the actinides. Early applications of this scheme were only applied to fit abundances up to the $A = 200$, where individual isotopic data are available. The challenge is to find some features which provide a measure of the accuracy for all nuclei beyond the $A = 195$ peak, including the unstable actinides in alpha-decay chains (Thielemann et al. 1993). In fact, there exist some observational constraints for these mass regions as well. Up to $A = 205$, isotopic abundances

stemming from the beta-decay of r -process progenitor nuclei (as in the lighter mass regions) are available. The r -abundances of the $^{206,207,208}\text{Pb}$ isotopes and ^{209}Bi contain additional information and are dominated by contributions from alpha-decay chains of isotopes with $A > 209$. For ^{206}Pb and ^{207}Pb , for example, β -decay from the r -progenitors back to these isotopes amounts to only 5%, whereas 95% of the r -abundances come from alpha back-decays of trans-lead isotopes. Similarly, for ^{208}Pb and ^{209}Bi the pure β contribution is about 15% and 7%.

In Figure 1 we show the results of our calculations before and after considering beta-decay and alpha-decay chains with short half-lives. The dashed and solid lines shown for $A > 206$ make both use of the mass model ETFSI-Q, but with slightly different superposition weights $\omega(n_n)$ (discussed below) in order to indicate an uncertainty range in the abundance predictions. For the nuclei ^{232}Th , ^{235}U , ^{238}U , and ^{244}Pu this range is indicated by a vertical bar. As demonstrated earlier by Pfeiffer et al. (1997), the theoretical prescription described above provides predictions in excellent agreement with the observed solar abundances (small filled circles in Figure 1), especially also for $A > 195$. This is also the case for ^{203}Tl , ^{204}Hg , ^{205}Tl , as well as for the alpha-decay dominated Pb and Bi isotopes from $A=206$ to 209. The r -contributions based on different s -process studies are listed in the first part of Table 1. Käppeler et al. (1989) made use of the classical model of an exponential superposition of neutron exposures, aiming for a best fit of pure s -nuclei. Beer et al. (1997) is based on stellar sites (thermal pulses with ^{13}C and ^{22}Ne neutron sources).

While we see appreciable variation between these two determinations of s -process contributions (and therefore r -process residuals) for $A=203$, 204, and 205, we see a much larger variation in the results of r -process calculations when utilizing different mass models. Although we will later employ dominantly the ETFSI-Q mass model (for the good reasons seen in Figure 1 and to be discussed below), we show in Table 1 predictions for ^{203}Tl , ^{204}Hg ,

^{205}Tl , $^{206-208}\text{Pb}$, and ^{209}Bi based on a large variety of mass formulas and models. The mass region 203-205 is one of those locations before and after r -process peaks, where too strong shell closures far from stability lead to "abundance troughs" or holes (see e.g. Chen et al. 1995 and Pfeiffer et al. 1997). The Hilf et al. (1976) droplet model with schematic shell corrections did this part reasonably well, although deviations of a factor of 3 can occur for $A=205$. The Finite Range Droplet Model with microscopic shell corrections (Möller et al. 1995) and the ETFSI-1 (Aboussir et al. 1995) are known for their pronounced shell effects, also far from stability. This leads to the extremely large deviations of up to a factor of 34 and excludes these mass models for a reliable extrapolation into unknown territory for heavier nuclei. The Hartree-Fock-Bogoliubov calculations with Skyrme force SkP by Dobaczewsky et al. (1996) are a fully microscopic self-consistent calculations, where the shell quenching far from stability, close to the neutron drip-line, results from interactions of loosely bound neutrons with this neutron continuum. However, the disadvantage is that these highly advanced and computationally expensive calculations still assume spherical symmetry for all nuclei. Thus HFB/SkP cannot be a good overall representation for astrophysical applications yet. We see this by an up to a factor of 6 overprediction of nuclei in the mass range 203-205. Attempts to improve the global behavior of a mass model like FRDM with pronounced shell effects by cutting in HFB/SkP at shell closures have been undertaken by Chen et al. (1995) and are shown here as FRDM/HFB. We see an improvement in comparison to FRDM alone, but still large deviations.

The best and close agreement is found with ETFSI-Q (Pearson, Nayak, & Goriely 1996), the version of ETFSI-1 where a phenomenological quenching of shell effects was introduced, combined with a consistent treatment of deformation. In fact, ETFSI-Q is the only mass model which yields a very good agreement with r -abundances over the whole mass range (not only in the r -process peaks, avoiding large troughs before and after shell closures). This is the reason why an overall least square fit made sense (not only for the

three peaks, as in case of the other mass models). This is listed as a second entry ETFSI-Q (lsq.) and changes the coefficient and power in n_n for the superposition weight $\omega(n_n)$ (see above) to 9.85×10^6 and -0.296 . For the isotopic abundances in the range $A=125-209$, the deviations from solar r -abundances yield an uncertainty characterized by a reduced $\chi^2=0.76$, which indicates that the predicted values are not significantly statistically different from the observed solar system values, with deviations typically in the 10% range. In the 203-205 mass region the agreement is slightly worse, showing on average more a 20% deviation, about a factor of 2 larger than the ETFSI-Q entry, which resulted from a fit to the more certain r -process peak regions alone. This can also be seen in Figure 1, where both results are plotted (dashed and solid).

The r -process contributions for $^{206-208}\text{Pb}$ and ^{209}Bi are dominated by alpha-decay chains from heavier nuclei up to $A=255$. Therefore, they represent a major test for the accuracy of our predictions for the heaviest r -process nuclei in the actinide region. The solar r -process abundances for ^{206}Pb and ^{207}Pb are quite well understood due to precision neutron capture cross sections which enter s -process studies (15-19% accuracy, Käppeler et al. 1989). This is somewhat worse for ^{209}Bi (43%), where the uncertainty range for the r -contribution lies within 64 and 92% of the solar abundance (Käppeler et al. 1989; Beer, Corvi, & Mutti 1997). For ^{208}Pb , which is dominated by the quite uncertain strong s -process component, Käppeler et al. (1989) determined the s -contribution to be 93.5%, Beer et al. (1997) 89%, while stellar site related calculations (Gallino 1998, private communication) seem to be able to contribute as much as 97%. This leaves for the r -process contribution between 3 and 11%, i.e. a mean value of 7% with a 57% uncertainty. Summarizing this part on the r -process abundances, suggests that $A=206$ and 207 provide clean r -process abundances with 15-19% accuracy, while $A=208$ and 209 have to be taken with some caution. This means that two of the four alpha-decay chain abundances from heavier r -process nuclei are well constrained and two other alpha-decay chains can be taken as a

consistency check. We have not listed here the analysis of Goriely (1997), because it suffers from uncertainties at the edge of fitting intervals (discussed above) and does not take into account the knowledge that the r -process contributions behave smoothly as a function of isotopic mass (see Käppeler et al. 1989). The latter is observed for the global mass range of heavy r -process nuclei beyond the $A=80$ peak and not expected to break down for masses beyond $A=200$, which also leads to smooth variations when distributed over the decay products of four alpha-decay chains.

When comparing in Table 1 the solar r -abundances of the nuclei 206 to 209 with predictions from different mass models, we obtain an additional and crucial test for their application in predicting actinide abundances. While the Hilf model was behaving reasonably in the 203-205 mass region, which tested mostly shell effects, it shows deviations up to a factor of 6 for these Pb and Bi abundances and is therefore not usable for reliable actinide predictions. The mass models FRDM and ETFSI-1, which already showed problems with shell effects for 203-205, also lead to an appreciable underprediction for 206-209 (up to a factor of 3). The hybrid model FRDM+HFB shows improved results, but deviations by a factor of 2 are still observed. This improves further with HFB/SkP, but the known deficiency of this purely spherical approach (plus its problems for 203-205) leave some doubts in its predictability. Only ETFSI-Q and ETFSI-Q (lsq) show an overall good performance. ETFSI-Q is actually better with a typical 10-20% accuracy. This leaves us with the conclusion that applications to actinide predictions make sense in the sequence ETFSI-Q and ETFSI-Q(lsq) (which are consistent with the solar r -abundances within the given errors), with the possible inclusion of FRDM/HFB and maybe HFB/SkP. The other models listed in Table 1 did not pass the test to reproduce the "actinide decay products" $A=206-209$. The fact that we can reproduce the solar Pb and Bi r -abundances, produced mainly by four different alpha-decay chains from the heavy mass region beyond $A = 209$ up to about 256, where (apart from Th and U) no "observables" exist to tune our fits, gives

us confidence that we are correctly predicting the radioactive actinide abundance values as well.

In fact, our results demonstrate that all possible observables related to actinide abundances are satisfied with an extension of components up to n_n of 3×10^{27} , obeying the same power laws for ω and τ as before. (At 3×10^{27} the abundance pattern is converged, a further extension to higher neutron densities has no effect, as the weights become so small that such components do not contribute.) This has the advantage that no additional parameter (like an upper limit for n_n components) is required. The remaining abundances of ^{232}Th ($\tau_{1/2}=1.405 \times 10^{10}\text{y}$), ^{235}U ($\tau_{1/2}=7.038 \times 10^8\text{y}$) and ^{238}U ($\tau_{1/2}=4.468 \times 10^9\text{y}$) will then, after their production, decay on their long decay-times. The abundances of ^{232}Th , ^{235}U , ^{238}U , and ^{244}Pu have already been shown in Table 1 and 2 of Pfeiffer et al. (1997) for most of the same mass models and will not be repeated here, with the exception of ^{232}Th which is used later for the Th/Eu chronometer.

Beta-delayed fission during the r -process was neglected in the calculations, because earlier investigations (Thielemann, Metzinger, & Klapdor 1983; Cowan et al. 1987; Thielemann, Cameron, & Cowan 1989; Cowan, Thielemann, & Truran 1991), when constrained by experimental data (Hoff 1986, 1987), have shown that to first order fission is unimportant. After the end of the r -process we considered spontaneous fission for nuclei beyond $A = 256$ (i.e., ^{256}Cf) and the few known nuclei undergoing spontaneous fission for $A < 256$. Their fission products will make no contribution to the mass range $A=232-255$ (which includes the Th and U isotopes). Therefore, only nuclei with $A \leq 255$ were included in the decay chains. We want to state again that the correct prediction for the r -process contribution to the $A=206, 207, 208, \text{ and } 209$ nuclei, produced mostly by alpha-decay chains starting in the mass region $A=232-255$, gives a strong indication that the total amount of matter in the $A=232-255$ mass range is well predicted within this model. While

extrapolations always involve some risk, the pleasing agreement noted here for four different alpha-decay chains suggests that our calculations also have good predictive power in this region of the nuclear chart.

To summarize this section, the excellent fit of our calculations to the solar system isotopic abundance distribution for $A > 130$ suggests that one type of astrophysical event has been responsible for r -process production throughout this mass range. We cannot yet identify what type of event that was, but we expect that the processed matter experienced a smoothly varying set of thermodynamic and neutron density conditions, which led to such a good agreement with solar r -abundances. We caution the reader that our insufficient knowledge of the properties of nuclei far from stability could contribute to uncertainties in the abundance predictions for the chronometer elements Th and U, but by performing numerous tests, we examined the nuclear physics input which best reproduces all observables (including also the $A=206-209$ nuclei that most constrain the interesting radioactive mass region). These tests (to be discussed further in §4.2) also reveal a clearly indicated error range.

3. Abundance Comparisons

We next compare our theoretical r -process calculations with solar system r -process and stellar elemental abundance distributions. In Figure 2 we consider abundance data for the ultra-metal-poor star CS 22892-052 ($[\text{Fe}/\text{H}] \simeq -3.1$).⁸ The observations from Sneden et al. (1996) are indicated by large filled squares, while the small squares are the solar system

⁸We adopt the usual spectroscopic notations that $[A/B] \equiv \log_{10}(N_A/N_B)_{\text{star}} - \log_{10}(N_A/N_B)_{\odot}$, and that $\log \epsilon(A) \equiv \log_{10}(N_A/N_H) + 12.0$, for elements A and B. Also, metallicity will be arbitrarily defined here to be equivalent to the stellar $[\text{Fe}/\text{H}]$ value.

r -process abundances connected by a dashed line. The solar elemental abundances are of course sums over the isotopic abundances, and these are based on deconvolving the total solar system abundances (Anders & Ebihara 1982, Anders & Grevesse 1989) into s - and r -process abundance fractions using the neutron capture cross sections of Käppeler et al. (1989) and Wisshak et al. (1996; see also Sneden et al. 1996 and Burris et al. 1998 for details). The solid line in Figure 2 indicates the predicted abundances from the ETFSI-Q calculations. Both the solar data and the predicted r -process abundances have been scaled vertically downward to account for the much lower metallicity of this star with respect to the sun. It is clear from the figure that the stellar data, the scaled solar abundances and the theoretical r -process abundances are coincident, at least for the stable elements Ba ($Z = 56$) and above.

Figure 3 shows abundances for the very metal-poor ($[\text{Fe}/\text{H}] = -2.7$) halo giant HD 115444. It includes the ground-based data (an average of the observational values from Griffin et al. 1982 and Gilroy et al. 1988; see also Sneden et al. 1998) indicated by open squares, while HST data from Sneden et al. (1998) are indicated by solid squares. In this figure we also include a new abundance value for thorium and an upper limit (as an arrow) on uranium. These radioactive elements will be discussed in §4. While Os was detected with somewhat large error bars in CS 22892-052, there are much more extensive 3rd r -process peak data available for HD 115444 (due to the HST observations). Sneden et al. (1998) have shown the similarity between the solar system r -process elemental curve and the data (both ground-based and space-based) all the way through the 3rd r -process peak for this star. Our new r -process calculations (the solid line in the figure) further confirm this result.

Figure 4 illustrates abundances for HD 122563, a star of approximately the same metallicity as HD 115444. However, HD 122563 is much less abundant in neutron-capture elements than is HD 115444, and only upper limits (indicated by arrows) for the 3rd

r -process peak elements were obtained by Sneden et al. (1998). The ground-based data are averages of a number of studies (as discussed in Sneden et al. 1998). Both the solar system scaled r -process curve and our new r -process calculations are consistent with the available ground-based data and the upper limits for HD 122563 for elements with $Z \geq 56$.

The fourth halo star for which there are extensive data is HD 126238. This star with a metallicity of $[\text{Fe}/\text{H}] = -1.7$ is more metal-rich than the previously discussed stars. Cowan et al. (1996) and Sneden et al. (1998) have reported HST detections of the 3rd r -process peak elements along with Pb in this star, and those data are plotted in Figure 5. We again see the similarity in the abundance pattern for the heaviest neutron-capture elements in this star and the scaled solar r -process abundances, both predicted by our calculations and by actual solar data. There is, however, some deviation between the Ba abundance (a predominantly s -process element) and the r -process curves, which may indicate the onset of Galactic s -processing already at this higher metallicity (see also Cowan et al. 1996, Sneden et al. 1998), which agrees well with chemical evolution expectations. It is possible that some s -processing might have contributed also to the Pb abundance, although our data are not adequate to show such an enhancement.

The overall r -process to Fe ratio at low metallicities is highly variable. This was first noted by Gilroy et al. (1988), and is certainly evident in the four stars considered here. Specifically, the $[\text{Eu}/\text{Fe}]$ ratio is +1.56 in CS 22892–052 (Sneden et al. 1994), +0.70 in HD 115444 as found in this paper, –0.44 in HD 122563 (Gratton & Sneden 1994) and +0.17 in HD 126238 (Gratton & Sneden 1994). Burris et al. (1998) will discuss this phenomenon more extensively. These results demonstrate that individual r -process events are resolved, on time scales probably shorter than Galactic mixing time-scales, but that the r -process abundances in each event are apparently well reproduced by a solar r -composition.

4. Chronometers

Actinide chronometers have been used to determine Galactic ages by (i) predicting $^{232}\text{Th}/^{238}\text{U}$ and $^{235}\text{U}/^{238}\text{U}$ ratios in r -process calculations, (ii) applying them in Galactic evolution models, which include assumptions about the histories of star formation rates and r -process production, and finally (iii) comparing these ratios with meteoritic data, which provide the Th/U and U/U ratios at the formation of the solar system. Low-metallicity stars have the advantage that one can avoid uncertainties introduced by chemical evolution modeling. The metallicities of the halo stars for which neutron-capture element data have become available range from $[\text{Fe}/\text{H}] = -3$ to about -2 . Typical (Galactic chemical) evolution calculations suggest *roughly* the "metallicity-age" relation $[\text{Fe}/\text{H}] = -1$ at 10^9y , -2 at 10^8y , and -3 at 10^7y (see e.g., Chiappini et al. 1997, Tsujimoto et al. 1997). Even if this estimate is uncertain by factors of 2-3, very low metallicity stars most certainly were born when the Galaxy was only $10^7 - 10^8\text{y}$ old, a tiny fraction of the present age of the Galaxy. Thus the neutron-capture elements observed in very low metallicity stars were generated in one or at most a few prior nucleosynthesis episodes. If several events contributed, the time interval between these events had to be very short in comparison to thorium decay ages. Thus, no error is made by simply adding these contributions, without considering decays, and treating them as one abundance distribution which undergoes decay until the present time. Any prior Galactic evolution can therefore be treated as a single r -process event incorporated into the observed star.

4.1. New Observations

Snedden et al. (1996) used the technique described above in deriving a thorium-based age for CS 22892-052. Detailed analyses for other low metallicity stars with high neutron-capture element abundance levels would further strengthen the reliability of such age

determinations. An obvious candidate is HD 115444. It is about 0.3 dex more metal-rich than CS 22892-052, and has more moderate overabundances of neutron-capture elements (e.g., $[\text{Eu}/\text{Fe}] \simeq +0.7$). However, it is an easier star for detailed spectroscopy, as it is much the brighter star ($V = 9.0$ against 13.1 for CS 22892-052). Therefore new ground-based UV and blue spectra of HD 115444, having high resolution ($R \simeq 50,000$ to 60,000) and high S/N ($\simeq 75$ to 200 near $\lambda 4000 \text{ \AA}$), have been gathered with the McDonald Observatory 2.7m telescope and 2D-coudé spectrograph (Tull et al. 1995) and the Keck I HIRES (Vogt et al. 1992). An extensive analysis of the McDonald spectrum of this star is in preparation (Westin et al. 1999); here we discuss preliminary analysis of only the chronometer elements.

In Figure 6 we show small spectral regions surrounding two Th II lines and one U II line in our data. The observed spectra are co-added data from the Keck and McDonald raw spectra; significant noise reductions in the spectra were achieved by the averaging of the spectra. Superimposed on each observed spectrum are four synthetic spectra in which only the abundance of thorium or uranium has been allowed to vary. To compute these synthetic spectra, we employed the current version of the line analysis code of Sneden (1973). We adopted the model atmosphere for HD 115444 derived by Pilachowski et al. (1996); the atomic/molecular line lists for each spectral region are described briefly below.

The Th II line at $\lambda 4019.13 \text{ \AA}$ in HD 115444 is easily seen in the observed spectrum displayed in the top panel of Figure 6. The contaminating absorptions to this complex feature are also apparent. We used the line list described in Sneden et al. (1996), which was based on earlier studies of François et al. (1993) and Morell et al. (1992), but here we added two ^{13}CH lines to the list. Norris, Ryan, & Beers (1997) have demonstrated that there are possibly severe blending complications to the Th II feature caused by these ^{13}CH lines (see their Figure 1). The ^{13}CH contamination is greatest in those halo giants with either strong CH bands and/or low $^{12}\text{C}/^{13}\text{C}$ ratios. From analysis of ^{12}CH and ^{13}CH

lines in other spectral regions, we estimate $^{12}\text{C}/^{13}\text{C} \simeq 7\text{--}8$ for HD 115444. The overall CH band strength was a free parameter that was adjusted to match the ^{13}CH doublet at $\lambda\lambda 4020.0, 4020.2 \text{ \AA}$, and then the ^{13}CH absorption at $\lambda 4019 \text{ \AA}$ was determined by this band strength, the transition probability ratio between the relevant ^{12}CH and ^{13}CH lines, and the $^{12}\text{C}/^{13}\text{C}$ ratio. The major remaining contamination of the Th II feature is due to Co I (chiefly at $\lambda 4019.3 \text{ \AA}$); and we altered the assumed Co abundance to match this absorption. Finally, we call attention to the partial Nd II blend at $\lambda 4018.84 \text{ \AA}$; its strength in our HD 115444 spectrum is well matched by the Nd abundance recommended in earlier analyses of this star (Griffin et al. 1982, Gilroy et al. 1988). With these features accounted for, the remaining absorption near $\lambda 4019 \text{ \AA}$ is attributed to Th II, and we deduced $\log \epsilon(\text{Th}) = -2.1 \pm 0.1$, the uncertainty being a combination of goodness-of-fit, continuum placement, and blending agent uncertainties.

Having a such good resolution and low noise spectrum of this star, we conducted a search for other strong Th II transitions. This exercise proved mostly fruitless, yielding only a possible line at $\lambda 4086.52 \text{ \AA}$ that is more than 4 times weaker than the $\lambda 4019 \text{ \AA}$ line. The observed spectrum given in the middle panel of Figure 6 shows no obvious Th II absorption. Nevertheless, we constructed a line list for features near the $\lambda 4086 \text{ \AA}$ line from Kurucz’s extensive atomic and molecular line lists (see Kurucz 1995a,b for descriptions of these data), and altered the transition probabilities to provide acceptable matches to the spectrum of the similar metallicity giant HD 122563; see Westin et al. (1999) for a more complete description. Application of this line list to predict the HD 115444 spectrum yielded the synthetic spectra in the middle panel of Figure 6. We could deduce only an upper limit to the thorium abundances here: $\log \epsilon(\text{Th}) \leq -2.2$.

We tried to identify lines of uranium in the HD 115444 spectrum. Our brief reconnaissance produced only a potentially detectable U II feature at $\lambda 3859.58 \text{ \AA}$. Again, no

absorption is obvious in the observed spectrum (bottom panel, Figure 6). Using the same procedure as we did for the Th II $\lambda 4086 \text{ \AA}$ line, we created a line list for this spectral region and computed synthetic spectra for HD 115444. From the observed/synthetic spectrum comparison, we suggest that $\log \epsilon(\text{U}) \leq -2.5$.

We also obtained McDonald and Keck I spectra at very high S/N for the bright, very metal-poor giant HD 122563. This star, however, is deficient in neutron-capture elements ($[\text{Eu}/\text{Fe}] \simeq -0.44$). We expected a weak-to-absent Th II $\lambda 4019 \text{ \AA}$ line, and found none in the observed spectrum. A synthetic spectrum computation yielded only that $\log \epsilon(\text{Th}) \leq -3.1$. A Keck spectrum was obtained for CS 22892-052, and although it has high resolution, the S/N is low. Therefore we chose to smooth this spectrum (sacrificing resolution for S/N) and then to merge it with the CTIO 4m echelle spectrum employed by Sneden et al. (1996). We again first derived $^{12}\text{C}/^{13}\text{C} \simeq 16$ (in excellent agreement with the estimate of Norris et al. 1997) from other CH features in the CS 22892–052 spectrum. Then analysis of the $\lambda 4019 \text{ \AA}$ blend suggested $\log \epsilon(\text{Th}) = -1.6 \pm 0.1$ (Sneden et al. derived -1.55 from just their CTIO spectrum, but see also Sneden et al. 1999 for additional abundance determinations for CS 22892–052.)

A summary of our new abundance results for HD 115444, HD 122563, and CS 22892-052 is given in Table 2. We also used synthetic spectrum computations of the strong Eu II lines at $\lambda\lambda 4129, 4205 \text{ \AA}$ to derive new values of the europium abundances in these stars. Our results here are in good accord with previous determinations (Griffin et al. 1982, Gilroy et al. 1982, Sneden et al. 1996, 1998). We have not obtained spectra of the radioactive elements in HD 126238, and thus this star will play no part in the age discussion to follow.

4.2. Ages

The agreement between the stable stellar abundances observed in low metallicity stars and the solar r -process abundances, demonstrates that these stars experienced only an r -process contribution for elements beyond Ba and that this contribution seems indistinguishable from a solar r -process mix. Thorium and uranium are produced solely in the r -process, but they are unstable and decay on long timescales. Knowing their production abundances in an r -process site and comparing them with the present observed abundances in a low metallicity star allows the stellar age to be determined (or the time when the pre-stellar cloud experienced the last pollution by r -process matter). For the cases with very low metallicities, these stars are expected to have formed not longer than 10^8 y after the formation of the Galaxy. Therefore, their ages are, within small uncertainties, identical to the age of the Galaxy.

With the robust fits between stable solar r -abundances and our theoretical r -process predictions as discussed in §2 and §3, we can also make use of the abundances of Th and U as predictions for the zero decay-age abundances of these radioactive elements. We have therefore compared our theoretical estimates for the initial radioactive abundances with observed abundances in the metal-poor halo stars. Recall from Figure 1, where the abundances were compared before and after decay, that the calculations match very well (after decay) all the stable r -process nuclei (even the heaviest Pb and Bi isotopes) in the solar system. That agreement strengthens our abundance predictions for the radioactive nuclei synthesized in the r -process.

The predicted Th/Eu ratio at zero decay-age, based upon the ETFSI-Q mass model and a superposition of components (see §2) according to a least square fit to solar r -abundances in the mass range 125-209, is 0.48 or $\log \epsilon(\text{Th}/\text{Eu})_0 = -0.32$. For the ETFSI-Q model the ratio is 0.546 or $\log \epsilon(\text{Th}/\text{Eu})_0 = -0.26$. We compared this value with the observed

$\log \epsilon(\text{Th}/\text{Eu})_*$ abundance ratios for the three very metal-poor halo stars HD 115444, CS 22892-052, and HD 122563 given in Table 2. Ignoring the case for HD 122563, where we only have an upper limit, we note that the Th/Eu ratios in the other two stars agree within observational uncertainties of $\sigma[\log \epsilon(\text{Th}/\text{Eu})]=\pm 0.08$. (See also Sneden et al. 1999.) Averaging their ratios (i.e., using $\log \epsilon(\text{Th}/\text{Eu}) = -0.63$), yields a lower limit for the average age of these very low metallicity stars of 13.8 Gyr. This results from the mere fact that the solar Th/Eu ratio listed in Table 3 (at the formation of the solar nebula 4.5 billion years ago) represents a lower limit to the zero decay-age r -process abundances, because Eu is stable and Th (although constantly produced and ejected into the interstellar medium) is partially decayed. Sneden et al. (1996) originally estimated an uncertainty in the $\epsilon(\text{Th}/\text{Eu})$ of ± 0.08 for CS 22892-052, which yielded an age uncertainty of about ± 3.7 Gyr. The only error sources considered then were observational/analytical uncertainties in the abundance determination. With two stars analyzed here, yielding essentially the same Th/Eu ratios, we estimate the uncertainties to be decreased slightly, and suggest an “observational” age uncertainty for the stellar pair to be ± 3.5 Gyr.

In Table 3 we also list results with zero decay-age Th/Eu ratios from our r -process calculations of §2, making use of a variety of nuclear mass models far from stability. Our “best” choice, ETFSI-Q, yields ages between 14.5 and 17.1 Gyr. Although not as easily obtainable as in the case of the observations, we also have to investigate the possible error due to the theoretical abundance predictions on which this age determination is based. We first test the agreement that is typical for stable isotopes and elements resulting from our abundance predictions with the ETFSI-Q nuclear input. The stable element Eu entering our age determination (later) has an observed solar system elemental abundance by number of 0.0907 ± 0.0032 (on a scale where $N(\text{Si}) = 10^6$). The different methods of determining the superposition weights $\omega(n_n)$, either via only adjusting to the r -process peaks or by performing a global fit, led to the two sets of abundance predictions ETFSI-Q and ETFSI-Q

(lsq). The ETFSI-Q (lsq) predicts an abundance for the element of 0.087, which agrees exactly within the deduced errors for r -process residuals. ETFSI-Q predicts 0.11533, which agrees within roughly 20%. For the isotopic abundances in the range $A=125$ – 209 , the deviations from solar r -abundances yield an uncertainty characterized by a reduced $\chi^2=0.76$, which indicates that the predicted values are not significantly statistically different from the observed solar system values. If instead we compare predicted and observed *elemental* abundances in the range $56 \leq Z \leq 83$, we find a reduced $\chi^2=0.86$, again reflecting good agreement and with deviations typically in the 10% range. Thus, making use of the two sets ETFSI-Q and ETFSI-Q (lsq), which differ in the Th/Eu production ratio by 13%, would seem to be sufficient to cover the uncertainty range.

It is also possible to estimate a possible error range by making use of other mass models. They have, however, to fulfill the test discussed in §2, based on the correct reproduction of the $A=206$ - 209 abundances, which are dominated by and thus are a measure of the decay-chain products of the actinides. This led to the exclusion of the mass models of Hilf, FRDM, and ETFSI-1. FRDM is listed in Table 3, but the Eu abundance prediction is off by a factor of more than 3, underlining the previous finding, and therefore making the age prediction meaningless. Our conclusion was that applications to actinide predictions only make sense within the sequence ETFSI-Q and ETFSI-Q(lsq) (which are consistent with the solar r -abundances within the given errors), with the possible inclusion of FRDM/HFB and maybe HFB/SkP. HFB/SkP, which already showed the worst agreement among this chosen set, and could not model deformed nuclei, gives an age prediction of 10.2 Gyr. This is smaller than the lower limit obtained with the solar Th/Eu ratio and can therefore be neglected as well. The average of ETFSI-Q and ETFSI-Q (lsq) and FRDM+HFB (which passed the test of Table 1 to reproduce the $A=203$ - 209 r -process abundances) is 15.6 Gyr. The range 13.8 to 17.1 of Table 3, which includes the (observational) lower limit from the solar Th/Eu ratio, can be somewhat generously assigned with an error of 2 Gyr. In

general the fit quality of our theoretical predictions for the isotopic abundances in the range $A=125\text{--}209$ gave a reduced $\chi^2=0.76$, which corresponds roughly to a 1σ error of $(1.00-0.76)\times 100 = 24\%$. When applying this 24% uncertainty to the (theoretical) Th/Eu ratio, this yields an age uncertainty of 3 Gyrs. Thus, 3 Gyr should be a safe assessment of the theoretical uncertainties involved in the Th/Eu chronometer ratio.

The combined error has to reflect this error, based on the theoretical uncertainties due to nuclear model predictions far from stability, and the observational error. Adding in quadrature the observational age uncertainty (as discussed above) to this uncorrelated theoretical uncertainty yields a total age uncertainty of approximately 4.6 Gyr, i.e. stellar ages of these low metallicity stars of 15.6 ± 4.6 Gyr. The estimated age remains virtually unchanged from our previous estimates (Cowan et al. 1997, Pfeiffer et al. 1997).

The uranium abundance in HD 115444 is a very weak upper limit, and in fact the value may be much lower. Nevertheless, we can make some age estimate based upon this upper limit. We note, however, that unlike the Th elemental abundance which depends only upon one isotope, the uranium abundance results from the decay of two radioactive isotopes with very different half-lives. In the ETFSI-Q model the initial elemental abundance is dominated by the shorter half-life isotope, ^{235}U , while presumably the elemental abundance in the metal-poor stars is mostly determined by ^{238}U . Ignoring the initial ^{235}U production entirely (this isotope decays in much less than a Hubble time), and only comparing the initial time-zero ^{238}U and the observed upper limit in HD 115444 gives a lower limit on the age of this star of > 7.1 Gyr. While this age estimate has much observational and theoretical uncertainty, it is entirely consistent with the value found using the Th abundance.

5. Discussion and Conclusions

The abundance comparisons shown in the figures indicate several striking results. First, as noted already by Sneden et al. (1998), for the four metal-poor stars for which extensive data have become available, the stellar data are in solar r -process proportions (at least for $Z \geq 56$). While this has been suggested now for a number of years, this trend is now seen over a wider elemental range, including data from the 3rd r -process peak, than was previously attainable. Future observations including Pb and Bi data, which are dominated by alpha decay-chains from actinide nuclei, would give further support for the method applied in this paper, where we have emphasized the use of theoretical r -process calculations in order to obtain zero decay-age abundances of Th. Furthermore, the fact that all four stars, covering a wide range of metallicities ($[\text{Fe}/\text{H}] = -3.1$ to -1.7), show the same consistent scaled solar r -process pattern, make other explanations (such as a random superposition of varying r -process abundances from different r -process sites with varying conditions, see e.g., Goriely & Arnould 1997) much less likely than a continuous set of conditions reproducing solar r -abundances in each single site. For elements with $Z \geq 56$, the relative elemental r -process abundances appear not to have changed over the history of the Galaxy. This further suggests that there is one r -process site in the Galaxy, at least for those elements.

However, the trend for the lighter neutron-capture elements with $A < 100$ is not as clear, but may be explainable in terms of the emergence of the weak s -process with increasing metallicity. The abundance values of Zr and Ge, for example, are approximately the same in HD 115444 and HD 122563, two stars of the same metallicity but which show large differences in the absolute levels of heavy neutron-capture elements. The weak s -process is expected to be metallicity dependent as a secondary process, but to occur earlier than the main s -process component, as it is produced in (core He-burning of) massive stars

rather than (He-shell flashes of) low/intermediate mass stars. We note, however, that it is unclear how effective the weak s -process might be in stars of extremely low metallicity, and other explanations may be possible. One such possibility may be that there are two r -process signatures – one for the lighter and one for the heavier r -process nuclei – reflecting two separate sites (Wasserburg, Busso, & Gallino 1996; Qian, Vogel, & Wasserburg 1998). (See Wheeler, Cowan, & Hillebrandt 1998, and Freiburghaus et al. 1999 for a discussion of possible second sites.) It is also conceivable that this region of Sr-Zr could be produced by a combination of the r - and the weak s -process, as suggested for the star CS 22892–052 by Cowan et al. (1995). Clearly more observational and theoretical work will be required to understand the production of these lighter n -capture elements early in the history of the Galaxy.

The detection of thorium in very metal-poor stars (pioneered by François, Spite, & Spite 1993) has provided the exciting opportunity of directly determining stellar ages (see Sneden et al. 1996, Cowan et al. 1997 and Pfeiffer et al. 1997). In this paper we have used the stable stellar and solar data to constrain the predicted (zero decay-age) values of the radioactive r -process nuclei. With detailed Th II analyses now in two very metal-poor stars, we have extended our previous age determinations to give an average age estimate of about 15.6 Gyr for very old halo stars, supporting previous age estimates for CS 22892–052 from Cowan et al. (1997) and Pfeiffer et al. (1997). Recent age determinations with the aid of the Re/Os chronometer (Takahashi et al. 1998) yield very similar ages and uncertainty ranges. The advantage of much better (by now experimentally) known nuclear properties and missing observational uncertainties is compensated in the Re/Os chronometer by the uncertainties involved in galactic evolution and the temperature history of matter in stars and the interstellar medium. The latter is missing here because, after an initial r -process injection, only Th decay has to be accounted for.

It is also encouraging to note that our new age estimate for these two stars is consistent with recent globular cluster age determinations based upon Hipparcos data (see Pont et al. 1998). We note further the consistency of this age estimate with the recent cosmological age estimates, based upon high-redshift supernovae, of 14.9 ± 1.5 Gyr (Perlmutter et al. 1999) and 14.2 ± 1.7 Gyr (Riess et al. 1998). We caution, however, that there are still several uncertainties which limit the accuracy of these radioactive age determinations. In particular, small changes in the abundance determinations can result in large age uncertainties due to the exponential decay-time dependence. The resulting age similarities for the two stars for which data are available, however, do lend support to using this technique, which we emphasize is independent of chemical evolution models. To refine further and strengthen this technique will require many more observations of the long-lived radioactive elements in other metal-poor halo stars. Additional theoretical calculations, employing full, dynamic r -process calculations, suitable for astrophysical environments, will also be needed to make more accurate stellar and Galactic age determinations.

We thank John Norris and Jim Lawler for helpful conversations, and appreciate the expert help of the STScI staff in all aspects of the planning and execution of the observations over three HST Cycles. We also thank an anonymous referee who helped us to improve the paper, especially on the treatment of the nuclear uncertainties. Further thanks go to P. Möller for the QRPA code, M. Pearson for the ETFSI-Q masses, and B. Neas and L. D. Cowan, Dept. of Biostatistics and Epidemiology at OUHSC, for helpful advice on statistics and uncertainties. Support for this work was provided through grants GO-05421, GO-05856, and GO-06748 from the Space Science Telescope Institute, which is operated by the Association of Universities for Research in Astronomy, Inc., under NASA contract NAS5-26555. Support was also provided by the National Science Foundation (AST-9314936 and AST-9618332 to J.J.C.), (AST-9315068 and AST-9618364 to C.S.) and (AST-9529454

to T.C.B.), by the Swiss Nationalfonds (grants 20-47252.96 and 2000-53798.98), and by the German BMBF (grant 06Mz864) and DFG (grant Kr8065). J.J.C. and F.-K.T. thank the Institute for Theoretical Physics at the University of California at Santa Barbara, for partial support from the National Science Foundation under Grant No. PHY94-07194. This work was completed while J.J.C. was in residence at the University of Texas at Austin, funded through the University of Oklahoma as a Big XII Faculty Fellow; we are very grateful to both institutions for their support of this research.

REFERENCES

- Aboussir, Y., Pearson, J. M., Dutta, A. K., & Tondeur, F. 1995, *At. Data Nucl. Data Tables*, 61, 127
- Anders, E., & Ebihara, M. 1982, *Geochim. Cosmochim. Acta*, 46, 2363
- Anders, E., & Grevesse, N. 1989, *Geochim. Cosmochim. Acta*, 53, 197
- Beer, H., Corvi, F., Mutti, P. 1997, *ApJ*, 474, 8437
- Burris, D. L., Pilachowski, C. A., Armandroff, T., Sneden, C., & Cowan, J. J. 1998, in preparation
- Chen, B., Dobaczewski, J., Kratz, K.-L., Langanke, K., Pfeiffer, B., Thielemann, F.-K., & Vogel, P. 1995, *Phys. Lett.*, B355, 37
- Chiappini, Matteucci, & Gratton, 1997, *ApJ*, 477, 765
- Cowan, J. J., Burris, D. L., Sneden, C., McWilliam, A., & Preston, G. W. 1995, *ApJ*, 439, L51
- Cowan, J.J., Sneden, C., Truran, J. W., & Burris, D. L. 1996, *ApJ*, 460, L115
- Cowan, J.J., Thielemann, F.-K., & Truran, J.W. 1991, *Phys. Rep.*, 208, 267
- Cowan, J.J., McWilliam, A., Sneden, C., & Burris, D. L. 1997, *ApJ*, 480, 246
- Dobaczewski, J. et al. 1996, *Phys. Rev.*, C53, 2809
- Fogelberg, B. et al. 1998, in *ENAM 98, Exotic Nuclei and Atomic Masses*, ed. B. Sherrill, AIP, in press
- François, P. & Gacquer, W. 1999, in *Nuclei in the Cosmos V*, ed. N. Prantzos, Gif-sur-Yvette:Editions Frontieres:), in press

- François, P., Spite, M., & Spite, F. 1993, *A&A*, 274, 821
- Freiburghaus, C., Rembges, J.-F., Rauscher, T., Thielemann, F.-K., Kratz, K.-L., Pfeiffer, B., & Cowan, J. J. 1999, *ApJ*, in press
- Gilroy, K. K., Sneden, C., Pilachowski, C. A., & Cowan, J. J. 1988, *ApJ*, 327, 298
- Goriely, S. 1997, *A&A*, 327, 845
- Goriely, S., & Arnould, M. 1996, *A&A*, 312, 327
- Goriely, S., & Arnould, M. 1997, *A&A*, 322, L29
- Gratton, R., & Sneden, C. 1991, *A&A*, 241, 501
- Gratton, R., & Sneden, C. 1994, *A&A*, 287, 927
- Griffin, R., Griffin, R., Gustafsson, B., & Vieira, T. 1982, *MNRAS*, 198, 637
- Hoff, R. 1986, in *Weak and Electromagnetic Interactions in Nuclei*, ed. H.V. Klapdor (Heidelberg: Springer), 207
- Hoff, R. 1987, *J. Phys. G.*, 24, S343
- Isakov, V.I. et al. 1998, in *ENAM 98, Exotic Nuclei and Atomic Masses*, ed. B. Sherrill, AIP, in press
- Käppeler, F., Beer, H., & Wisshak, K. 1989, *Rep. Prog. Phys.*, 52, 945
- Käppeler, F. 1998, in *Nuclei in the Cosmos V*, in press
- Kratz, K.-L., Thielemann, F.-K., Hillebrandt, W., Möller, P., Harms, V., & Truran, J. W. 1988, *J. Phys. G*, 14, 331

- Kratz, K.-L., Bitouzet, J.-P., Thielemann, F.-K., Möller, P., & Pfeiffer, B. 1993, ApJ, 403, 216
- Kratz, K.-L. 1998, in *ENAM 98, Exotic Nuclei and Atomic Masses*, ed. B. Sherrill, AIP, in press
- Kurucz, R. L. 1995a, in *Astrophysical Applications of Powerful New Databases*, PASP Conf. Ser. 78, eds Adelman, S. J. & Wiese, W. L. (San Francisco, ASP), 205
- Kurucz, R. L. 1995b, in *Laboratory and Astronomical High Resolution Spectra*, PASP Conf. Ser. 81, eds Sauval, A. J., Blomme, R., & Grevesse, N., (San Francisco, ASP), 583
- Mach, H. et al. 1998, in *ENAM 98, Exotic Nuclei and Atomic Masses*, ed. B. Sherrill, AIP, in press
- Magain, P. 1995, A&A, 297, 686
- Mathews, G. J., Bazan, G., & Cowan, J. J. 1992, ApJ, 391, 719
- McWilliam, A. 1997, ARAA, 35, 503
- McWilliam, A. 1998, AJ, 115, 1640
- McWilliam, A., Preston, G. W., Sneden, C., & Searle, L. 1995a, AJ, 109, 2736.
- McWilliam, A., Preston, G. W., Sneden, C., & Searle, L. 1995b, AJ, 109, 2757.
- Meyer, B. S. 1994, ARA&A, 32, 153
- Meyer, B. S., McLaughlin, G.C., & Fuller, G.M. 1998, Phys. Rev., C58, 3696
- Möller, P., Nix, J.R., Myers, W.D., & Swiatecki, W.J. 1995, At. Data Nucl. Data Tables 59, 185

- Möller, P., Nix, J.R., & Kratz, K.-L. 1997, *At. Data Nucl. Data Tables* 66, 131
- Möller, P., & Randrup, J. 1990, *Nucl. Phys.* A514, 1
- Morell, O., Källander, D., & Butcher, H. R. 1992, *A&A*, 259, 543
- Norris, J. E., Ryan, S. G., & Beers, T. C. 1997, *ApJ*, 490, L169
- Pearson, J. M., Nayak, R. C., & Goriely, S. 1996, *Phys. Lett.* B387, 455
- Perlmutter, S., et al. 1999, *Ap J*, in press
- Pfeiffer, B., Kratz, K.-L., & Thielemann, F.-K. 1997, *Z. Phys. A*, 357, 235
- Pilachowski, C. A., Sneden, C., & Kraft, R. P. 1996, *AJ*, 111, 1689
- Pont, F., Mayor, M., Turon, C., & Vandenberg, D. A. 1998, *A&A*, 329, 87
- Qian, Y.-Z., Vogel, P., & Wasserburg, G. J. 1998, *ApJ*, 494, 285
- Qian, Y.-Z., & Woosley, S. E. 1996, *ApJ*, 471, 331
- Ratzel, X. 1988, Diploma thesis, Karlsruhe
- Riess, A. et al. 1998, *AJ*, 116, 1009
- Seeger, P.A., Fowler, W.A., Clayton, D.D. 1965, *Ap.J. Suppl.*, 97, 121
- Sneden, C. 1973, *ApJ*, 184, 839
- Sneden, C., & Parthasarathy, M. 1983, *ApJ*, 267, 757
- Sneden, C., & Pilachowski, C.A. 1985, *ApJ*, 288, L55
- Sneden, C., Preston, G. W., McWilliam, A., & Searle, L. 1994, *ApJ*, 431, L27

- Sneden, C., McWilliam, A., Preston, G. W., Cowan, J. J., Burris, D. L., & Armosky, B. J. 1996, *ApJ*, 467, 819
- Sneden, C., Cowan, J. J., Burris, D. L., & Truran, J. W. 1998, *ApJ*, 496, 235
- Sneden, C. et al., 1999, in preparation
- Spite, M., & Spite, F. 1978, *A&A*, 67, 23
- Takahashi, K., Faestermann, T., Kienle, P., Bosch, F., Langer, N., Wagenhuber, J. 1998, in *9th Workshop on Nuclear Astrophysics*, eds. W. Hillebrandt, E. Müller, Max-Planck-Inst. für Astrophysic MPA/P10, p.175
- Takahashi, K., Witt, J., & Janka, H.-T. 1994, *A&A*, 286, 857
- Thielemann, F.-K., Cameron, A.G.W., Cowan, J.J. 1989, in *Fifty Years with Nuclear Fission*, ed. J. Behrens (American Nuclear Society), p.592
- Thielemann, F.,iburghaus, C., Kolbe, E., Rauscher, T., Rembges, F., Kratz, K.-L., Pfeiffer, B., Schatz, H., Wiescher, M., & Cowan, J.J. 1998, *Proc. Int. Conf. Gamma-Ray Spectroscopy and Related Topics*, eds. G. Molnar, T. Belgya, Zs. Révay, Springer Hungarica, p.521
- Thielemann, F.-K., Bitouzet, J.-P., Kratz, K.-L., Möller, P., Cowan, J. J., Truran, J. W. 1993, *Phys. Rep.*, 227, 269
- Thielemann, F.-K., Kratz, K.-L., Pfeiffer, B., Rauscher, T., van Wormer, L., & Wiescher, M. 1994, *Nucl. Phys. A*, 570, 329c
- Thielemann, F.-K., Metzinger, J., Klapdor, H.V. 1983, *Z. Phys.*, A309, 301
- Truran, J. W. 1981, *A&A*, 97, 391

- Tsujimoto, T., Yoshii, Y., Nomoto, K., Matteucci, F., Thielemann, F.-K. & Hashimoto, M. 1997, ApJ, 483, 228
- Tull, R. G., MacQueen, P. J., Sneden, C., and Lambert, D. L. 1995, PASP, 107, 251
- Vogt, S. S. 1992, in ESO Workshop on High Resolution Spectroscopy with the VLT, ed. M. H. Ulrich (ESO, Garching), p. 223
- Wasserburg, G.J., Busso, M., & Gallino, R. 1996, ApJ, 466, L109
- Westin, J., Sneden, C., Edvardsson, B., Gustafsson, B. & Cowan, J. J. 1999, in preparation
- Wheeler, C., Cowan, J. J., & Hillebrandt, W. 1998, ApJ, 493, L101
- Wisshak, K., Voss, F., & Käppeler, F. 1996, in Proceedings of the 8th Workshop on Nuclear Astrophysics, ed. W. Hillebrandt, & E. Müller (Munich: MPI), 16
- Woosley, S. E., Wilson, J. R., Mathews, G. J., Hoffman, R. D., & Meyer, B. S. 1994, ApJ, 433, 229

Table 1. Isotopic r-Abundances in Pb-Region (in 10^{-3})

Model	^{203}Tl	^{204}Hg	^{205}Tl	^{206}Pb	^{207}Pb	^{208}Pb	^{209}Bi
Solar r-Abundances							
Käppeler	12±6	20±2	41±15	223±43	280±47	118±167	93±12
Beer	19±6	25±6	34±15	256	228	198	134
combined	16±8	21±6	38±21	240±61	254±66	158±236	114±17
Calculations (Fit to 3 r-Process Peaks)							
Hilf	7.5	25.1	13.7	53.5	44.7	36.3	39.5
FRDM	2.4	1.3	1.2	77.4	81.2	46.4	69.6
ETFSI-1	3.2	2.7	2.9	80.3	82.2	69.5	56.1
HFB/SkP	44.5	131.3	54.1	190.9	140.6	162.6	99.0
FRDM/HFB	13.2	3.6	2.3	112.1	114.9	73.8	101.2
ETFSI-Q	10.7	20.6	19.4	199.3	184.1	170.3	129.8
Calculations (Least Square Fit A=125-209)							
ETFSI-Q	8.5	16.4	15.4	157.9	146.2	135.2	102.9

Table 2. Neutron-Capture Element Abundances

Transition	log ϵ HD 115444	log ϵ CS 22892-052	log ϵ HD 122563
Derived Abundances			
Th II $\lambda 4019 \text{ \AA}$	-2.1	-1.6	<-3.1
Th II $\lambda 4086 \text{ \AA}$	<-2.2
U II $\lambda 3860 \text{ \AA}$	<-2.5
Eu II $\lambda \lambda 4129, 4205 \text{ \AA}$	-1.5	-0.9	-2.6
Abundance Ratios			
Th/Eu	-0.6	-0.66	<-0.5
U/Eu	<-1.0
Th/U	>+0.4

Table 3. Th/Eu Chronometers

Model	${}_{90}\text{Th}$	${}_{63}\text{Eu}$	$\frac{\text{Th}}{\text{Eu}} _{model}$	Age [Gyrs]
Solar	0.042	0.09	0.463	13.8
FRDM	0.04280	0.02420	1.7695	41.0
ETFSI-1	0.02949	0.06041	0.4881	14.9
HFB/SkP	0.01991	0.05134	0.3879	10.2
FRDM+HFB	0.03449	0.06958	0.4957	15.2
ETFSI-Q	0.06292	0.11533	0.5456	17.1
ETFSI-Q(lsq)	0.04222	0.08788	0.4804	14.5

Figure Captions:

Fig. 1.— Comparison of theoretical abundances prior to and after beta- and alpha-decay with solar r -process abundances (small filled circles). For $A > 206$ two superposition weights $\omega(n_n)$ have been utilized, obtained from fitting the r -process abundance peaks (ETFISI-Q, dashed) and from a global abundance fit in the mass region $A = 125-209$ (ETFISI-Q lsq., solid). The solid vertical lines show the calculated abundance range within ETFISI-Q and ETFISI-Q (lsq) predictions for the nuclei ^{232}Th , ^{235}U , ^{238}U and ^{244}Pu . (See text for discussion.)

Fig. 2.— Comparison of observed abundances (large filled squares) from CS 22892-052 and solar r -process abundances (small filled circles) joined by a dashed line with a theoretical r -process abundance distribution denoted by a solid line. (See text for discussion.)

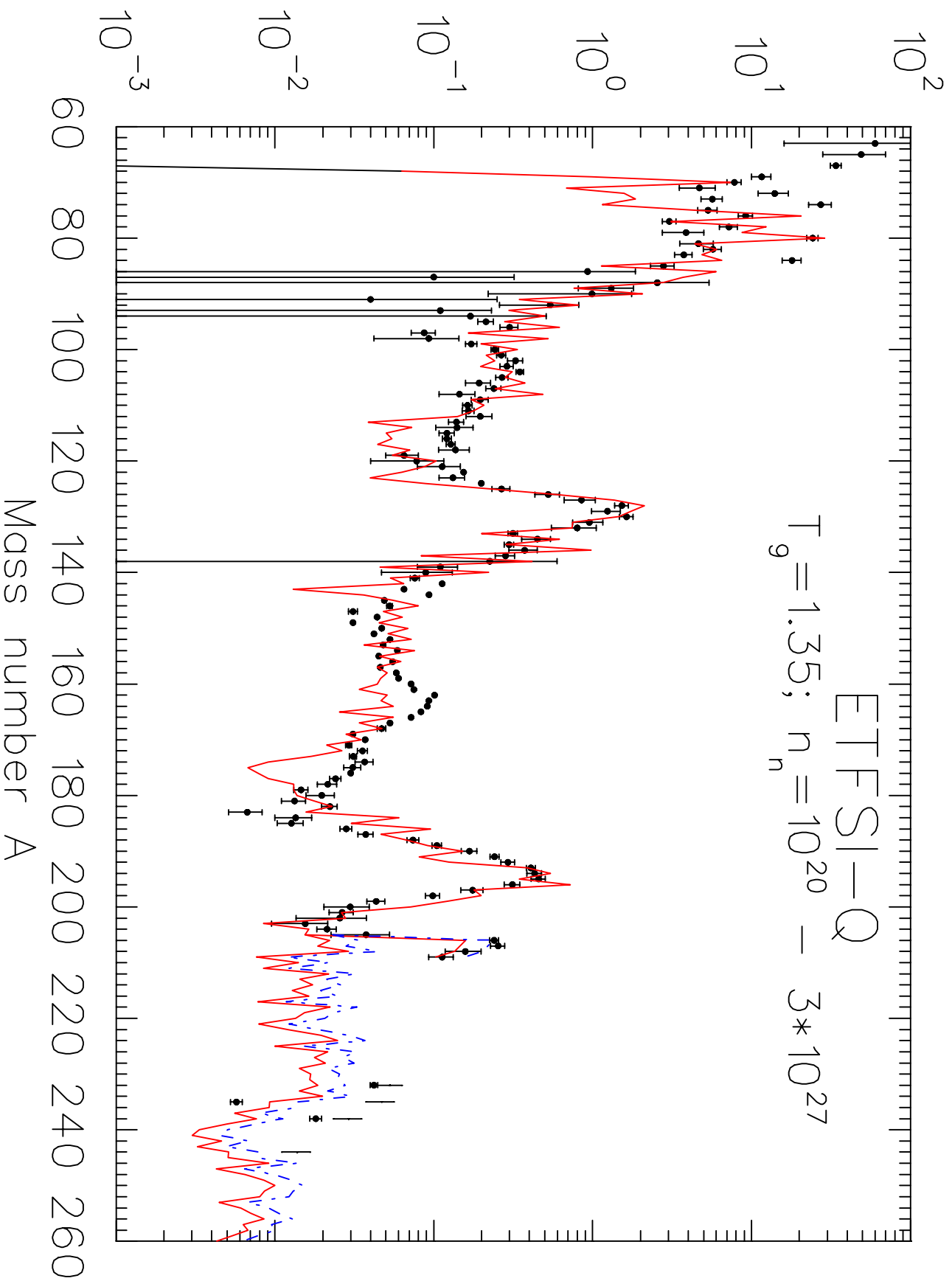
Fig. 3.— An abundance comparison between the neutron-capture elements in HD 115444 and a theoretical r -process (solid line) and a solar system r -process (dashed line) abundance distribution. Ground-based data (from various sources, see text for discussion) are indicated by open squares, while HST data from Sneden et al. (1998) are indicated by solid squares.

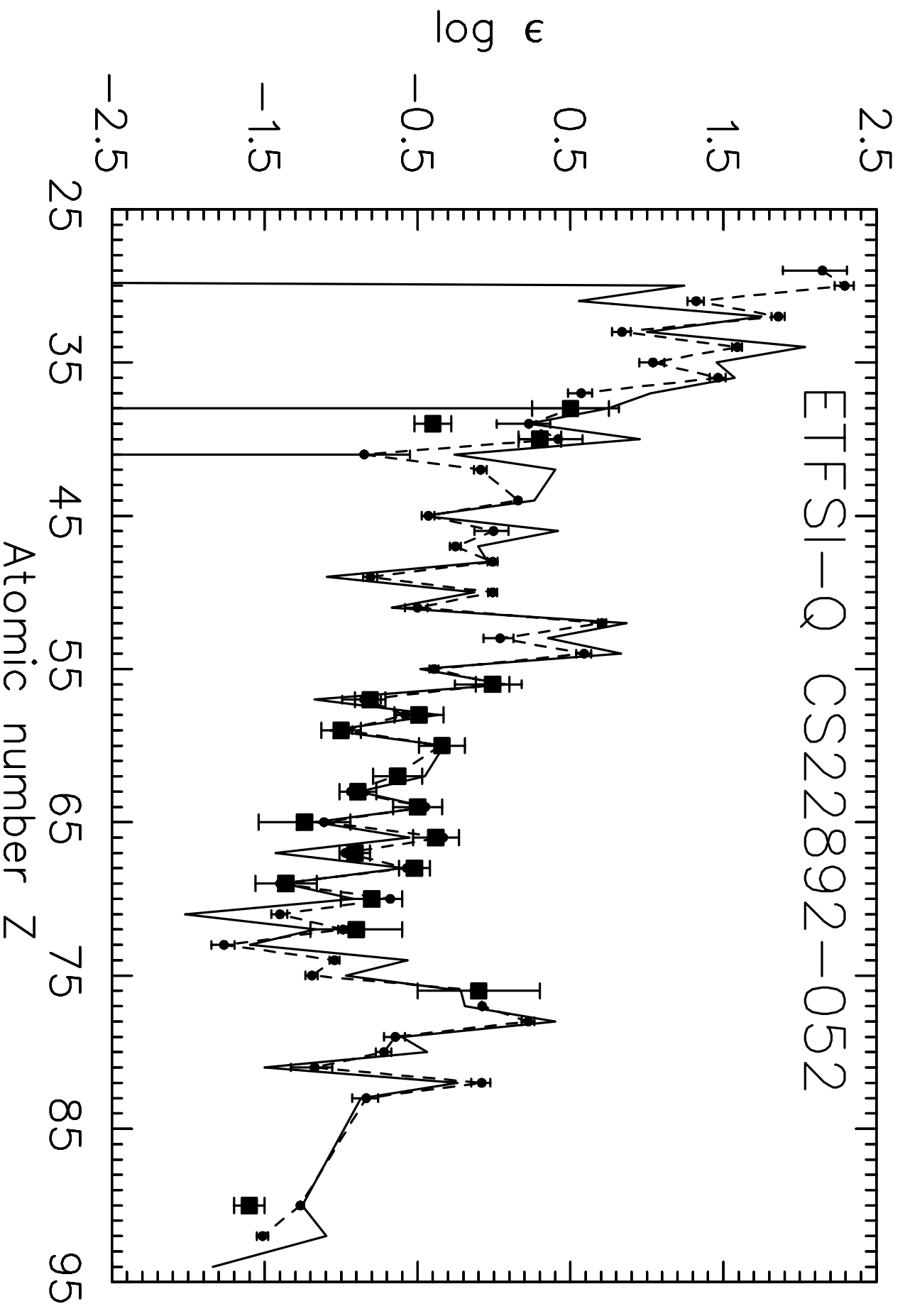
Fig. 4.— An abundance comparison for HD 122563 in the same style as that of Figure 3. Upper limits for Os and Pt are indicated by crosses with attached arrows.

Fig. 5.— An abundance comparison for HD 126238 in the same style as that of Figure 3.

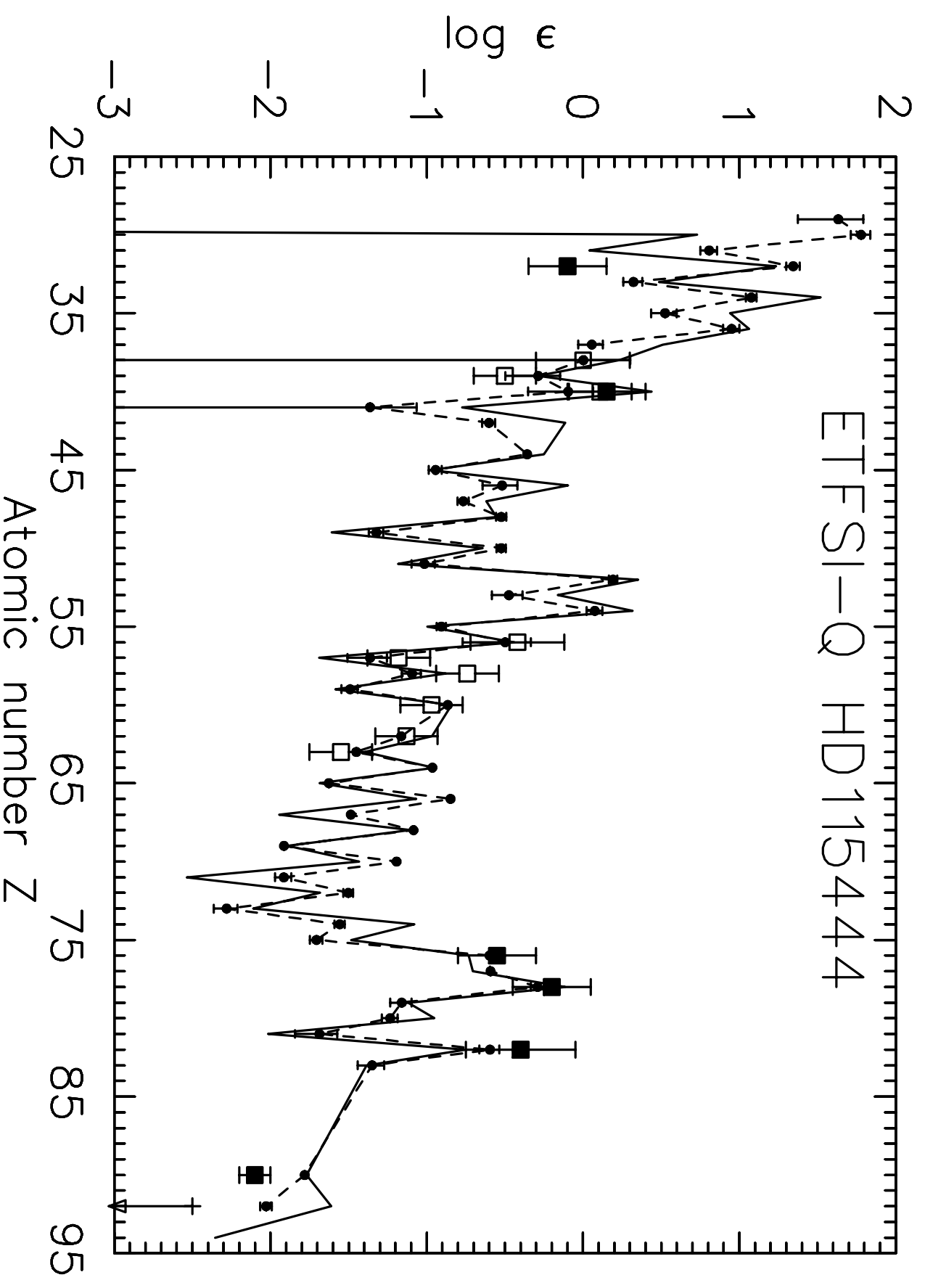
Fig. 6.— Observed and synthetic spectra of thorium and uranium transitions in the spectrum of HD 115444. See text for discussion of the observational data and the synthetic spectrum computations.

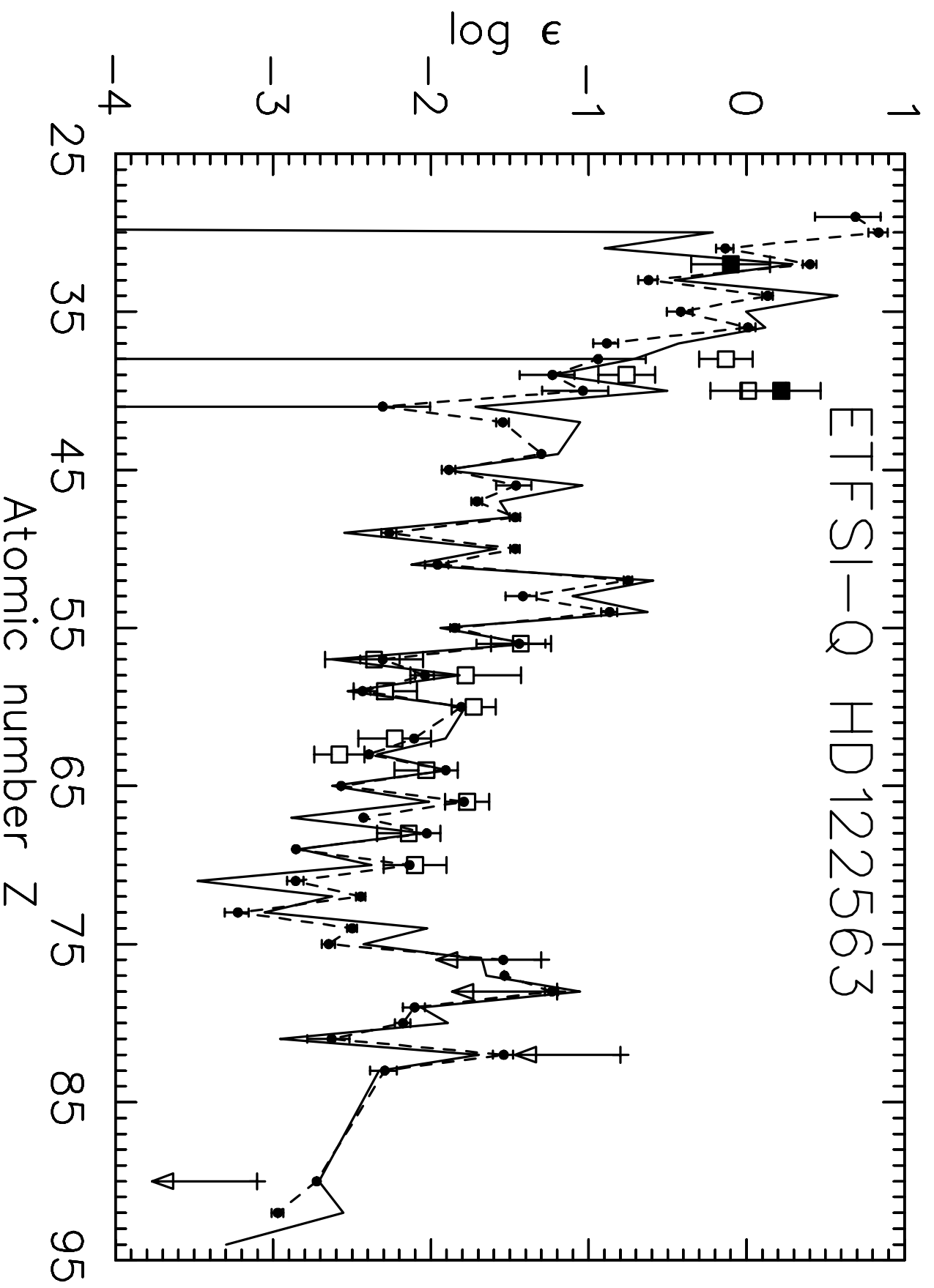
Solar r-abundance





ETFSl-Q HD115444





ETFSI-Q HD126238

